



# Modelling droplet size distributions in polydispersed wet-steam flows

A.J. White<sup>a,\*</sup>, M.J. Hounslow<sup>b</sup>

<sup>a</sup>*School of Engineering, University of Durham, South Road, Durham DH1 3LE, UK*

<sup>b</sup>*Chemical and Process Engineering, University of Sheffield, Mappin Street, Sheffield S1 3JD, UK*

Received 7 July 1999; received in revised form 6 September 1999

## Abstract

A method is presented for modelling droplet size distributions within condensing steam flows. Polydispersed droplet spectra are treated by modelling moments of the size distribution, rather than the more traditional approach of discretising the continuous range of radii. Attention is focussed on wet-steam flow in turbines for which accurate prediction of droplet spectra is an essential step towards computing thermodynamic wetness losses and other two-phase effects. The method has been validated by comparison with independent calculations for both primary and secondary nucleation. Excellent agreement was obtained throughout, but with substantial reduction in complexity and computer usage. The moment equations have been cast in both Lagrangian and Eulerian forms and are well suited for incorporation into computational fluid dynamic codes. © 2000 Elsevier Science Ltd. All rights reserved.

*Keywords:* Condensation; Wet-steam; Size distribution; Two-phase flow

## 1. Introduction

Vapour–droplet flows containing polydispersed liquid droplets are relevant to a number of areas of scientific and engineering importance. These include the flight of aircraft in humid conditions, wet-steam flows in steam turbines, and droplet-spray combustion processes. The work described in this paper stems from wet-steam research, but the methods presented may equally be of interest for other vapour–droplet flows with phase change.

For the large low-pressure (LP) turbines used for electricity generation, the presence of condensation leads to problems of blade erosion and to a loss in turbine efficiency. The latter stems from the irreversibil-

ities associated with phase transition, and from the impact of inter-phase heat and mass transfer on the flow behaviour. Each of these processes is strongly dependent on the size of the tiny liquid droplets which are formed by spontaneous nucleation from the vapour. Fig. 1 shows the entropy increase (computed with an established method [1]) for an initially wet flow undergoing a typical LP turbine blade-row expansion. The entropy is plotted in non-dimensional form as a function of initial droplet diameter, and the curve highlights the importance of droplet size in determining thermodynamic losses. This fact has not yet been taken on-board by turbine manufacturers who, for want of a suitable alternative, continue to use a purely empirical correlation to account for wetness losses. Measurements of droplet sizes in turbines, based on light extinction techniques [2], indicate that droplets are in fact present with a range of sizes typically span-

\* Corresponding author.

**Nomenclature**

$\mathbf{c}$	droplet slip velocity	$u$	modulus of $\mathbf{u}$
$d$	droplet diameter	$V$	volume
$f$	droplet number density function	$\mathbf{x}=(x_1, x_2, x_3)$	position vector
$G$	droplet growth rate (i.e., $dr/dt$ following the droplet)	$y$	wetness fraction
$h$	specific enthalpy	$\Delta T$	vapour subcooling, $(T_s - T_g)$
$J$	nucleation rate per unit mass of mixture	$\gamma$	skewness of size distribution
$l_g$	mean free path of vapour molecules	$\lambda_g$	thermal conductivity of vapour
$n_T$	total number of droplets per unit mass of mixture	$\mu_j$	$j$ th moment of size distribution
$p$	pressure	$\rho$	density
$Pr_g$	vapour Prandtl number	$\sigma$	standard deviation, surface tension
$r$	droplet radius		
$R_g$	gas constant per unit mass		
$s$	specific entropy		
$\mathbf{S}$	vector area		
$t$	time		
$\mathbf{u} = (u_1, u_2, u_3)$	velocity vector		

*Subscripts and superscripts*

g	vapour phase
l	liquid phase
$j$	moment order
m	mixture quantity
s	saturation quantity
'	particle phase space
1, 2	upstream, downstream

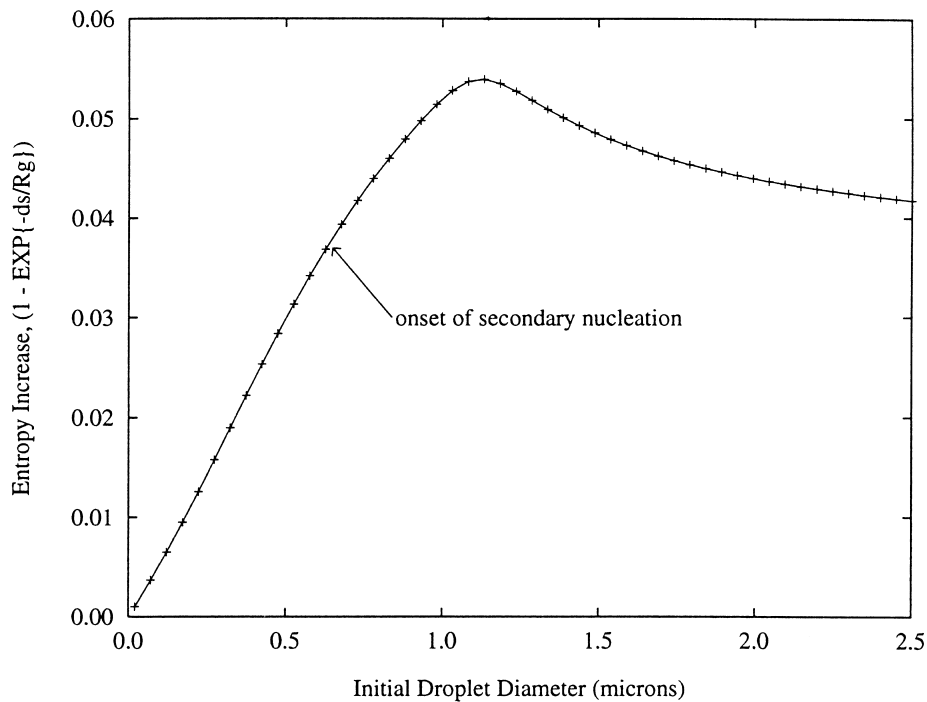


Fig. 1. Entropy increase as a function of initial droplet size for a wet-steam expansion (expansion rate,  $\dot{p} = 1500\text{s}^{-1}$ , initial wetness,  $y = 0.02$ , pressure ratio = 2.8).

ning one or two orders of magnitude and it is likely that this spread is even greater within nucleating regions of the flow. Since inter-phase heat and mass exchange are strong functions of droplet diameter, it is clear that the full spectrum of droplet sizes must be modelled in order to accurately predict two-phase behaviour.

To date, calculation methods for condensing steam flow have mostly followed a mixed Eulerian–Lagrangian approach, whereby conservation equations for the two-phase mixture are solved in an Eulerian frame of reference, but nucleation and droplet growth are calculated following fluid particles. Both steady and unsteady two-dimensional flows have been computed in this manner (see, for example, [1,3,4]) and in each case the continuous droplet spectra were modelled in a discrete fashion by computing the behaviour of a large number of droplet groups. Compared with the alternative fully Eulerian method, this type of calculation has a number of advantages which have been described in detail by Young [1]. Nonetheless, various difficulties arise since the method entails tracking streamlines through the flow-field and interpolating fluid properties between different computational grids. It is thus reasonable to suppose that the three-dimensional, unsteady flow-fields typical of LP turbines would be more easily computed in a purely Eulerian framework. (The difficulties for the mixed calculations are particularly severe for unsteady flows since the tracking procedures must then follow instantaneous fluid particle pathlines and the interpolation must be applied to droplet spectra in addition to the other fluid properties [4].) A few fully Eulerian methods have been reported in the literature, including those of Schnerr and Dohrmann [5] for two-dimensional moist air flow, and of McCallum and Hunt [6] for one-dimensional wet-steam flow, but none of the publications has presented a satisfactory means of dealing with the polydispersed liquid phase in an Eulerian framework. (In this connection, it is noted that both the methods cited employ averaging techniques which approximate the true polydispersed flow with a single droplet group.)

As stated above, polydispersed droplet and particle size distributions occur in many situations, and a variety of mathematical techniques have been developed to model them. These include the statistical approach often applied in atmospheric physics (e.g., [7,8]) and the moment evolution methods used, for example, to model growth and aggregation of kidney stones [9], and solids separation [10]. The present paper describes a method of treating wet-steam flows based on the latter, moment approach. Equivalent techniques have been employed in the past for other vapour–droplet flow problems (for example, for spray combustion processes [11]), but the moment method has not yet been formally applied to condensing flows. Unlike methods

based on an average droplet size, the moment approach correctly models exchanges of heat and mass between phases, but involves substantially less computation than discrete spectrum calculations. The moment equations may be cast in either a Lagrangian or an Eulerian form and are therefore readily incorporated into any computational flow method.

## 2. Theory

The conservation equations for condensing steam flow have been presented many times in the literature (e.g., [12]) and so the following theory will be restricted to droplet conservation. The techniques adopted broadly follow those developed for other size distribution problems (see, for example, [13,14]), but the equations are presented here in a form more appropriate to compressible vapour–droplet flows. It is assumed throughout that there is zero velocity slip between phases, which is an excellent approximation for most self-nucleating flows.

### 2.1. Droplet conservation for nucleating flows

Fig. 2 shows an arbitrary control volume drawn in “particle phase space”. This is a four-dimensional space composed of the three spatial dimensions,  $x_1$ ,  $x_2$  and  $x_3$  (only two of which are shown in the figure), and a particle size dimension,  $r$ . The trajectories of droplets in phase space are described by the phase vel-

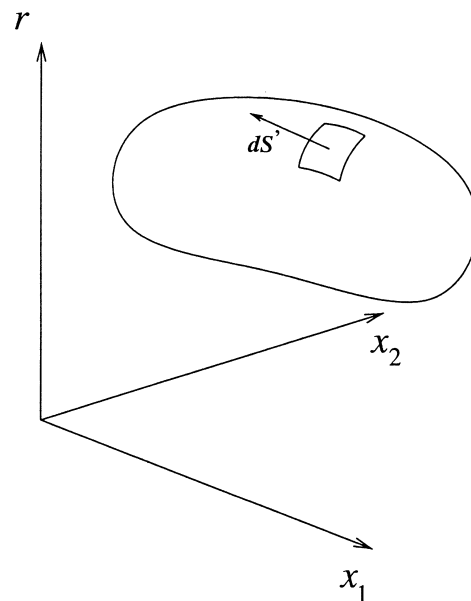


Fig. 2. Control volume in “particle phase space”.

ocity,  $\mathbf{u}'$ , comprising the three usual velocity components plus a droplet growth “velocity”. i.e.,

$$\mathbf{u}' = \begin{pmatrix} dx_1/dt \\ dx_2/dt \\ dx_3/dt \\ dr/dt \end{pmatrix} = \begin{pmatrix} u_1 \\ u_2 \\ u_3 \\ G \end{pmatrix}. \quad (1)$$

The phase velocity thus simultaneously describes the movement and growth of individual droplets.

The droplet size distribution varies continuously in time and space, and is described by the droplet number density function,  $f$ . Thus,  $f dr$  is the number of droplets per unit mass of mixture in the size range  $r$  to  $(r + dr)$ . The total number of droplets contained within the control volume of Fig. 2 is therefore

$$N_{cv} = \int \rho_m f dV' \quad (2)$$

where  $\rho_m$  is the mixture density and  $dV' = dx_1 dx_2 dx_3 dr$  is an elemental phase space volume.

With the above definitions, an expression for droplet conservation in integral Eulerian form is easily derived. Assuming no droplet breakup or agglomeration, changes in  $N_{cv}$  are due only to nucleation of new droplets within the control volume and to fluxes crossing the control surface. The latter include the usual convective fluxes plus an additional droplet growth flux, but with the mathematical formalism adopted here these fluxes may be treated in an identical manner. The droplet conservation equation is thus

$$\frac{\partial}{\partial t} \int \rho_m f dV' + \oint \rho_m f \mathbf{u}' \cdot d\mathbf{S}' = \int \rho_m J dV' \quad (3)$$

where  $J dr$  is the nucleation rate of droplets in the radius range  $r$  to  $(r + dr)$  per unit mass of mixture. (It should be noted that  $\rho_m$  and  $\mathbf{u}$  are functions of position and time, whilst  $f$ ,  $J$  and  $G$  also depend on the droplet radius.) The quantity  $d\mathbf{S}'$  is an element of control surface area. Although difficult to visualise, the meaning of  $d\mathbf{S}'$  should be clear by extension from three dimensions. By applying Gauss’s divergence theorem and shrinking to a point, Eq. (3) may be expressed in the differential form

$$\frac{\partial}{\partial t}(\rho_m f) + \nabla' \cdot (\rho_m f \mathbf{u}') = \rho_m J \quad (4)$$

where  $\nabla' = (\partial/\partial x_1, \partial/\partial x_2, \partial/\partial x_3, \partial/\partial r)^t$ .

The advantage of the phase space formulation is that it is easily extended to include other phenomena. For example, by writing  $f$  as a function of  $r$  and  $\mathbf{c}$ , where  $\mathbf{c}$  is the droplet slip velocity, inertial relaxation effects may be included without changing the form of Eq. (4) (although the number of dimensions would be increased to seven). However, for the current case,

with no velocity slip, it is convenient to expand Eq. (4) and revert to familiar physical space, giving

$$\frac{\partial}{\partial t}(\rho_m f) + \nabla \cdot (\rho_m f \mathbf{u}) + \frac{\partial}{\partial r}(\rho_m f G) = \rho_m J. \quad (5)$$

This is the Eulerian form of droplet conservation. So far, attempts at solving the equation in this form for wet-steam have resorted to a single average droplet size, and corresponding average growth rate.

## 2.2. Moment transforms

The use of moments for solving population balance problems brings a number of advantages which are discussed in Ref. [13, p. 51]. One benefit particularly relevant to wet-steam flow is that inter-phase heat and mass transfer may be accurately modelled by solving just a few moment equations, rather than by computing the formation and growth of a large number of droplet groups.

The  $j$ th moment of the droplet size distribution is defined as

$$\mu_j = \int_0^\infty r^j f dr \quad (6)$$

Low order moments have a physical significance and of particular interest here are the zeroth and third moments as these are related to the total number of droplets per unit mass of mixture and to the wetness fraction, respectively:

$$n_T = \mu_0 \quad (7)$$

$$y = \frac{4\pi\rho_1}{3} \mu_3. \quad (8)$$

Similarly, the first and second moments are related to the “total radius” and total droplet surface area. Since coupling between droplet conservation and the other conservation equations is chiefly through the wetness fraction (Eqs. (18) and (19) below), an expression is required for the variation of  $\mu_3$ .

The evolution of  $\mu_j$  may be determined from Eq. (5) by multiplying through by  $r^j$  and integrating over all radii. The last term on the LHS of Eq. (5) requires integration by parts. Noting that  $r^j f$  disappears at  $r = 0, \infty$ , the final result is

$$\begin{aligned} \frac{\partial}{\partial t}(\rho_m \mu_j) + \nabla \cdot (\rho_m \mu_j \mathbf{u}) \\ = j \rho_m \int_0^\infty r^{j-1} G f dr + \rho_m J_* r_*^j, \end{aligned} \quad (9)$$

or (by incorporating mass continuity) in Lagrangian form

$$\frac{D\mu_j}{Dt} = j \int_0^\infty r^{j-1} Gf dr + J_* r_*^j, \quad (10)$$

where  $D/Dt$  is the substantive derivative, following a fluid particle. In deriving these relations, it is assumed that droplets are formed only at the critical radius,  $r_*$ , so that the nucleation rate may be written as a Dirac-delta function:

$$J = J_* \delta(r - r_*), \quad (11)$$

where  $J_*$  is the rate of formation of critically-sized embryos per unit mass of mixture. Standard expressions are used for  $J_*$  and  $r_*$ , and these can be found in [15].

### 2.3. Closure of moment equations

Ideally, the moment evolution equations may be closed if droplet growth can be accurately represented by the linear relation

$$G = a_0 + a_1 r, \quad (12)$$

where  $a_0$  and  $a_1$  depend only on vapour properties. Under these circumstances, Eq. (10) would become

$$\frac{D\mu_j}{Dt} = j(a_0\mu_{j-1} + a_1\mu_j) + J_* r_*^j. \quad (13)$$

The rate of change of  $\mu_j$  thus depends only on  $\mu_j$  and  $\mu_{j-1}$ , and furthermore, this dependence disappears at  $j = 0$ . In other words Eq. (13) is a closed set of equations, requiring no extrapolation or additional modelling. Since the remaining gas dynamic equations may be solved once the wetness fraction is known, Eq. (13) suggests that only the first four moments need to be modelled in order to correctly compute all inter-phase exchange processes, provided Eq. (12) is a valid representation of droplet growth. Computing higher order moments, beyond  $j = 3$ , provides additional information on the shape of the size distribution, but does not affect the accuracy of the fluid dynamic calculations.

For drop-wise condensation in pure steam, droplet growth does not follow the linear relationship discussed above. However, for the size range of interest in turbine flows, the growth rate is accurately represented by (see Appendix):

$$G = \frac{a_{-1}}{r} + a_0 + a_1 r. \quad (14)$$

The counterpart of Eq. (13) now includes a dependence on  $\mu_{j-2}$ , which means the equations are no longer closed. In particular, the evolution of the 1st moment now depends on  $\mu_{-1}$ . However, the dependence is not strong and the problem may be overcome

with an appropriate extrapolation for  $\mu_{-1}$ . Further details of how this is achieved are given below.

### 2.4. Coupling with the gas dynamic equations

Although a major benefit of the moment approach is the ease with which it may be implemented in an Eulerian framework, the equations are developed in Lagrangian form here in order to compare with existing polydispersed calculation procedures. The gas dynamic equations are outlined below for completeness, but the reader is referred to [12] for a thorough derivation.

For inviscid, adiabatic wet-steam flow with zero inter-phase slip, the mass continuity, momentum and energy equations for the two-phase mixture are, respectively,

$$\frac{\partial \rho_m}{\partial t} + \nabla \cdot (\rho_m \mathbf{u}) = 0 \quad (15)$$

$$\rho_m \frac{D\mathbf{u}}{Dt} + \nabla p = 0 \quad (16)$$

$$\frac{\partial (\rho_m h_0)}{\partial t} + \nabla \cdot (\rho_m h_0 \mathbf{u}) - \frac{\partial p}{\partial t} = 0, \quad (17)$$

where  $h_0 = h_m + 1/2u^2$  is the mixture specific stagnation enthalpy. The enthalpy,  $h_m$ , and density,  $\rho_m$ , are mixture quantities and therefore depend on the wetness fraction according to the following expressions

$$h_m = (1 - y)h_g + yh_l \quad (18)$$

$$\frac{1}{\rho_m} = \frac{1 - y}{\rho_g} + \frac{y}{\rho_l} \simeq \frac{1 - y}{\rho_g} \quad (19)$$

Strictly, liquid-phase quantities, such as  $h_l$  and  $\rho_l$ , depend on the droplet radius due to capillarity effects [16]. However, experience has shown that this dependence may be neglected with virtually no change in the numerical results but with considerable reduction in complexity.

Introducing Eq. (15) into Eq. (17) and subtracting the dot product of  $\mathbf{u}$  and Eq. (16) gives the Lagrangian or thermodynamic form

$$\frac{Dh_m}{Dt} = \frac{1}{\rho_m} \frac{Dp}{Dt}. \quad (20)$$

(Note that this expression does not imply constant entropy of fluid particles, as it would for single-phase flow.)

Eqs. (8), (10), (18)–(20) together constitute a complete specification of changes in fluid properties following a fluid particle, and may be integrated if the

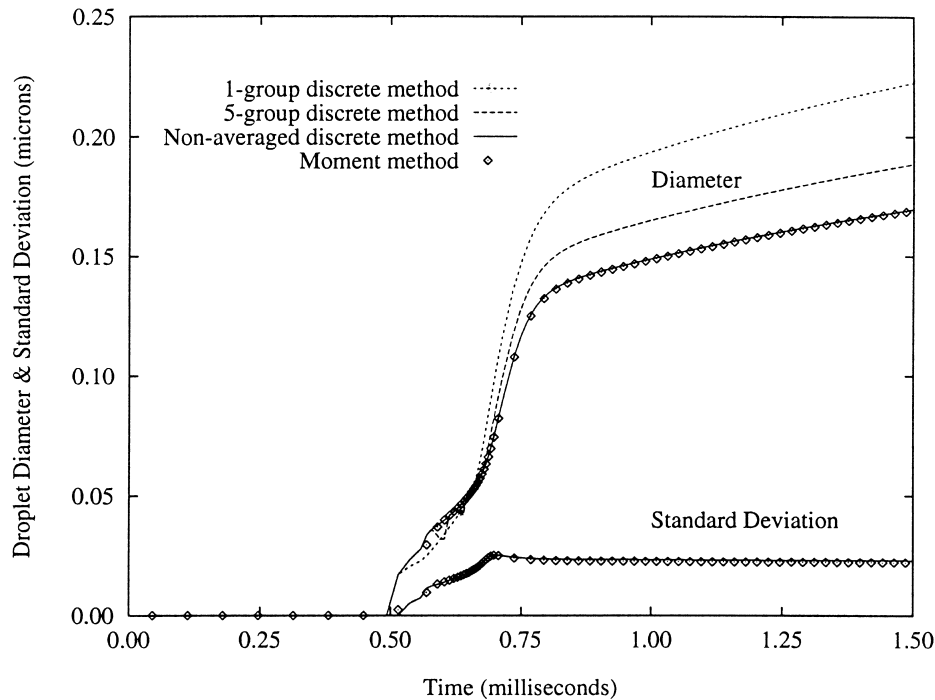


Fig. 3. Sauter mean droplet diameter and standard deviation computed for a nucleating expansion ( $\dot{p} = -1000$ ,  $\Delta T_1 = -5$ ,  $p_1 = 0.5$  bar).

pressure history,  $p(t)$ , is known. Details of the numerical procedure are not given here, but the approach is similar to that described in [1], and is based on a simple predictor–corrector method.

### 3. Comparison with existing methods

For the purpose of validation, the current method has been compared with a Lagrangian style discrete spectrum calculation procedure due to Young [1]. Since the aim here is to test the validity of the moment approach, and is not concerned with modelling the flow-field, the pressure–time history is specified by a simple, constant expansion rate, i.e.,

$$\dot{p} = \frac{1}{p} \frac{Dp}{Dt} = \text{constant}. \quad (21)$$

(The usual procedure is to determine  $p(t)$  by tracking fluid particles through a flow-field established by time-marching computations [1,3,4].)

Young's method originally employed the full droplet growth expression given in Appendix A, Eq. (A1).

However, the  $r_*/r$  term in the numerator of this expression stems from capillarity effects and is significant only in the very early stages of growth. Recent versions of Young's computer code do not, therefore, include this term, resulting in a growth expression which is adequately approximated by Eq. (12). The closed form of the moment evolution equation, Eq. (13), has therefore been used for an initial comparison, and results based on the full growth expression are deferred until later in this section.

#### 3.1. Primary nucleation

Fig. 3 compares the mean<sup>1</sup> and standard deviation of droplet diameters computed by the two methods for a nucleating expansion of initially dry steam. For accurate computation of the droplet spectrum, the discrete calculations may be carried out in a manner that retains every droplet group nucleated. However, this would lead to excessive computation for most practical flows (65 droplet groups were generated in the example shown), so the method may also be operated with a droplet averaging technique. The size range is then divided into a number of bins specified by the user, and at the end of each integration step, groups falling in the same bin are merged in a manner that conserves mass and droplet number. Curves are shown in the

<sup>1</sup> The mean size shown in this and subsequent figures is the Sauter mean diameter, defined as  $d_{32} = 2\mu_3/\mu_2$ .

figure for no averaging, five droplet groups, and a single droplet group. It is of some satisfaction that the moment approach produces results which are in excellent agreement with those obtained using the full spectrum, whereas the calculation with a single droplet group overestimates the average droplet size by approximately 30%. This discrepancy stems chiefly from the impact of averaging on the nucleation process, since it is principally the total number of droplets formed that dictates their final size. The inter-phase heat exchange rate cannot be correctly modelled with a single droplet group, leading to errors in the predicted vapour subcooling and, in turn, nucleation rate. Both the duration and intensity of the nucleation pulse are significantly affected, as shown in Fig. 4. (Note that the final droplet number differs by a factor of 2.4 between the 1-group and non-averaged cases.)

### 3.2. Secondary nucleation

The complex flows encountered in turbine blade passages involve a number of physical processes that may lead to a second, or even a third, nucleation of droplets. These include rapid re-expansion of an already wet flow, unsteady flow regimes induced by supercritical heat addition [17], and interaction between trailing-edge shock-waves and the nucleation zone [18]. For such cases, it is likely that correct modelling of the

droplet polydispersion will be even more important than for single-nucleation expansions, since established and freshly nucleated droplets may differ greatly in diameter.

Fig. 5 shows predicted droplet diameters for a rapid expansion with secondary nucleation. (The primary condensation has been modelled assuming a mono-dispersion of droplets.) The onset of the secondary nucleation is evident from the sudden reduction in average droplet diameter, due to the formation of many extremely small droplets. The moment method is again in very good agreement with calculations retaining the full droplet spectrum, and further evidence that the polydispersed nature of the flow is correctly modelled is given by the predicted skewness of the size distribution, defined by

$$\gamma = \frac{1}{n_T} \int_0^\infty \left( \frac{r - \bar{r}}{\sigma} \right)^3 f(r) dr. \quad (22)$$

This is also shown in the figure and compares extremely well with the discrete calculations. It is noted that monodispersed calculations give very significant errors for this case (as is also shown in Fig. 5), and correspondingly large inaccuracies for the vapour subcooling, entropy increase, and other fluid properties. (Other averaging techniques, preserving, for example, liquid mass and surface area, yield similarly inaccurate results.)

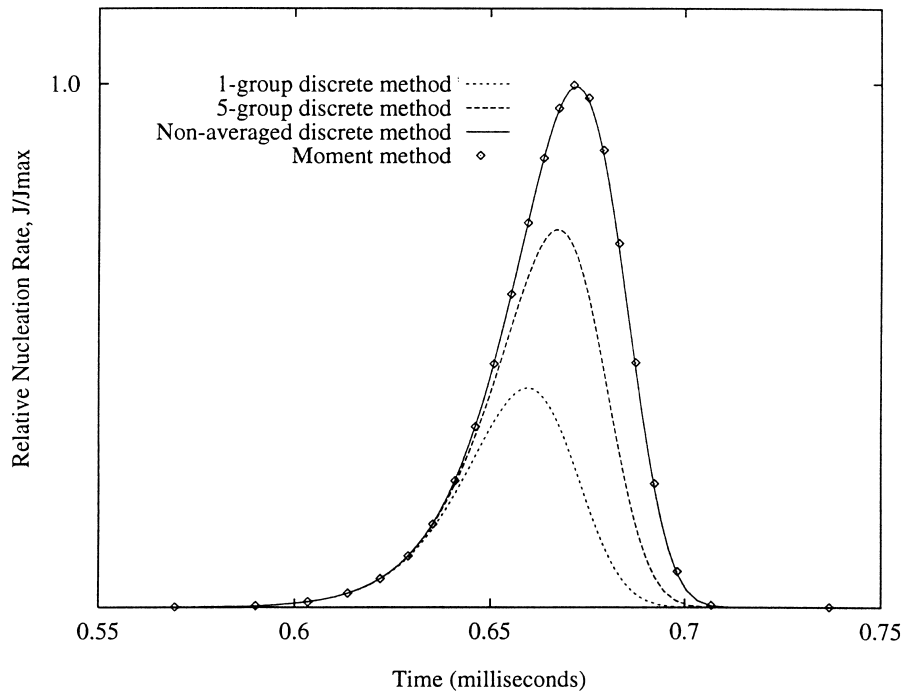


Fig. 4. Predicted nucleation pulses for the primary nucleating expansion of Fig. 3.

3.3. Inclusion of capillarity terms

As noted previously, inclusion of capillarity effects in the droplet growth law prevents complete closure of the moment evolution equations. This problem may be overcome if a suitable extrapolation is used to determine  $\mu_{-1}$ . A simple and robust estimation of this quantity can be obtained by considering a mono-dispersion with radius  $r_0$ , for which

$$\mu_{-1} = \frac{n_T}{r_0} = \frac{\mu_0^2}{\mu_1} \tag{23}$$

(Note that this corresponds to a linear extrapolation of  $\log \mu_j$ .) Fig. 6 shows predicted droplet sizes for both primary and secondary nucleating flows using the above estimation for  $\mu_{-1}$  combined with Eq. (14). The results are compared with discrete calculations based on the full droplet growth law, Eq. (A1). The approximation clearly works well for primary nucleation, but is less good in the nucleation zone of the secondary nucleating expansion. This is to be expected since the use of Eq. (23) then underpredicts  $\mu_{-1}$ . Improvements may be possible through the use of a more sophisticated extrapolation for  $\mu_{-1}$ , but the extra complexity seems unwarranted given the size of the discrepancies and the uncertainties which are inherent in droplet

growth theory anyway. (For a comprehensive discussion on the status of droplet growth theory, see [15].)

3.4. Higher order moments

Although only the first four moments of the size distribution are necessary to correctly model phase change, higher order moments are readily computed by solving one additional equation for each additional moment. The first nine moments, as predicted by both the discrete and moment methods, are plotted in Fig. 7 in the non-dimensional form:

$$\bar{\mu}_j = \frac{\mu_j}{\mu_{j+1} \mu_0} \tag{24}$$

(This form enables all the moments to be plotted on the same scale, and for a mono-dispersion yields  $\bar{\mu}_j = 1$  for all  $j$ .) Despite some discrepancies, the moment distribution is reasonably predicted for both primary and secondary nucleating cases.

If sufficient moments are computed, then it is theoretically possible to reconstruct the continuous size distribution using, for example, the methods described in [13]. This is unlikely to give reliable results for bimodal or complex size distributions, but for most purposes it is not necessary. Heat and mass transfer, entropy production rate, and other flow properties

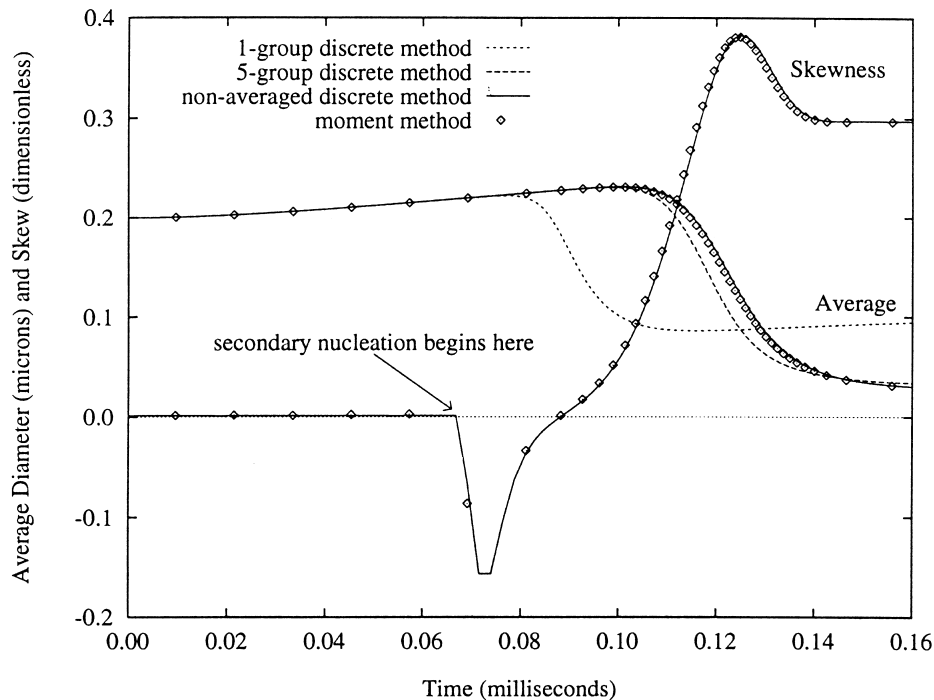


Fig. 5. Average droplet diameter and skewness for an expansion with secondary nucleation ( $\dot{p} = -10,000$ ,  $d_1 = 0.2 \mu\text{m}$ ,  $y_1 = 0.02$ ,  $p_1 = 0.25 \text{ bar}$ ). Values of skewness have been divided by 100.



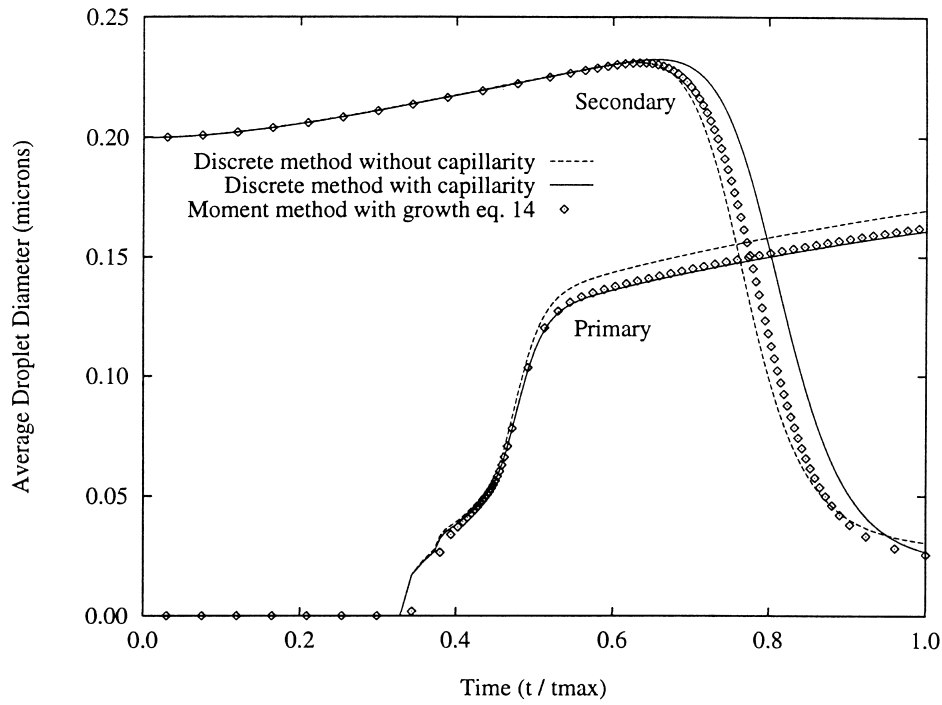


Fig. 6. Average droplet diameter predicted using different growth approximations — comparison of discrete and moment approaches.

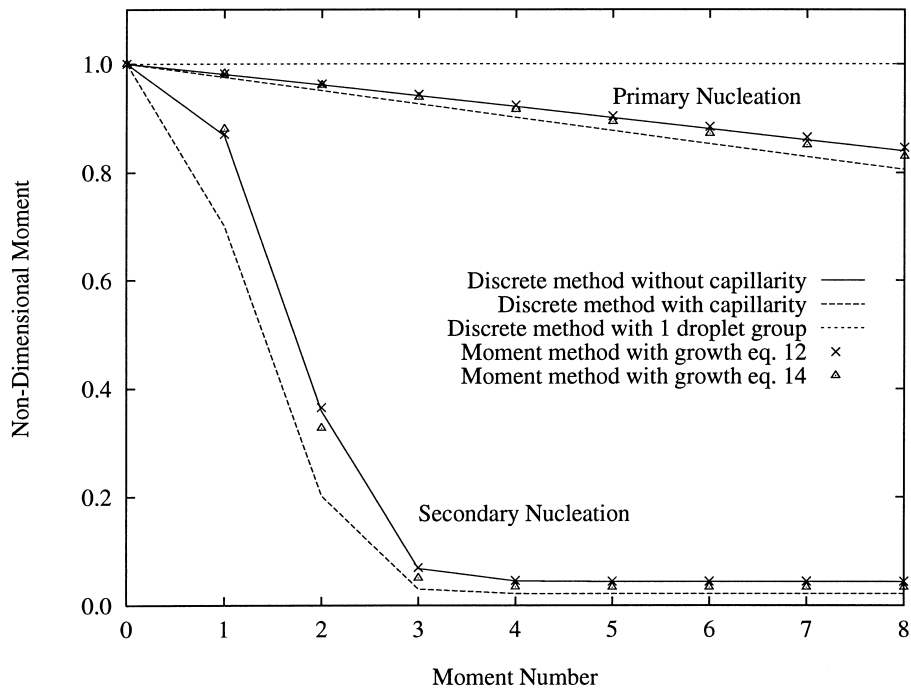


Fig. 7. The first nine moments of the size distribution for primary and secondary nucleating expansions.

may all be computed using just the first few moments, whilst the occurrence of phenomena such as secondary nucleation is easily identified from the average, standard deviation and skewness of the distributions. It may also be possible to model additional processes, such as droplet deposition onto turbine blades, using the moment approach, but this would require further investigation. If it is essential to compute the shape of the size distribution, it is probably safer, however, to resort to discrete calculations.

### 3.5. Comparison of CPU usage

Direct comparison of the CPU timings for the two methods is not possible because the computer program for the discrete method includes additional routines, for example to compute suitable time steps for stable integration. (The same time step sizes have been used for the moment calculations, but these are read as input to the computer program.) Nonetheless, it is clear from the timings, which are shown in Table 1, that the moment method affords considerable reductions in computational requirements and it would not be unreasonable to suppose an order of magnitude improvement over full spectrum calculations for typical cases.

## 4. Conclusions

A method of modelling droplet size distributions in condensing flows has been presented, and validated by comparison with an independent calculation procedure. The method is based on a moment transform of the droplet conservation equation, and produces results which are in excellent agreement with discretised calculations retaining the full droplet spectrum. The equations have been cast in a Lagrangian frame of reference for the purpose of validation, but the main advantage of the moment approach is that it may easily be implemented in an Eulerian framework and so lends itself well to CFD methods. This is in contrast to the discretised spectrum approach, for which Eulerian calculations would entail cumbersome spectrum

averaging techniques. The moment approach also requires considerably less computational effort than discrete calculations. Finally, it has been demonstrated that the use of a single droplet size (as is used for current Eulerian calculations) to approximate the true polydispersed flow, may lead to substantial errors, particularly in the case of secondary nucleations.

## Acknowledgements

The authors wish to thank Professor J.B. Young for kindly permitting the use of his Lagrangian wet-steam calculation procedures.

## Appendix. Droplet growth approximations

The droplet growth expression adopted as the basis of the current work is a slightly modified version of the standard Gyarmathy equation:

$$G = \frac{dr}{dt} = \frac{\lambda_g \Delta T (1 - r_*/r)}{\rho_1 (h_g - h_l) (r + 1.89(1 - \nu) l_g / Pr_g)}. \quad (\text{A1})$$

The factor  $(1 - \nu)$  is a semiempirical correction introduced by Young [15] to obtain precise agreement with experimental data for LP nozzle expansions.

The above expression may be approximated by expanding as a power series in  $r$ , giving

$$G = \sum_{n=-1}^{\infty} a_n r^n \quad (\text{A2})$$

where the  $a_n$  are functions only of the vapour properties and may be determined by straightforward manipulations. The agreement between the first three terms of Eq. (A2) and the full expression is shown in Fig. 8 for  $10^\circ$  subcooling and a pressure of 0.25 bar, i.e., at conditions typical of LP turbines. At higher pressures, the agreement for large radii deteriorates, but may be improved by including additional terms in the expansion. The moment equations must then be closed with appropriate extrapolations for the high order moments. However, this additional complexity is probably unjustified given the uncertainty in droplet growth theory. In the current work, therefore, only the first three terms of Eq. (A2) have been considered, leading to Eq. (14). Furthermore, the first of these terms only has a significant effect for the initial stages of growth and may be neglected without serious error. This leads to the linear growth law, Eq. (12).

Table 1  
Comparison of CPU timings on a Pentium II processor operating at 266 MHz

	Primary nucleation (s)	Secondary nucleation (s)
Full spectrum	4.40	17.29
5-Group	0.65	01.28
1-Group	0.34	00.28
Moments	0.06	00.07

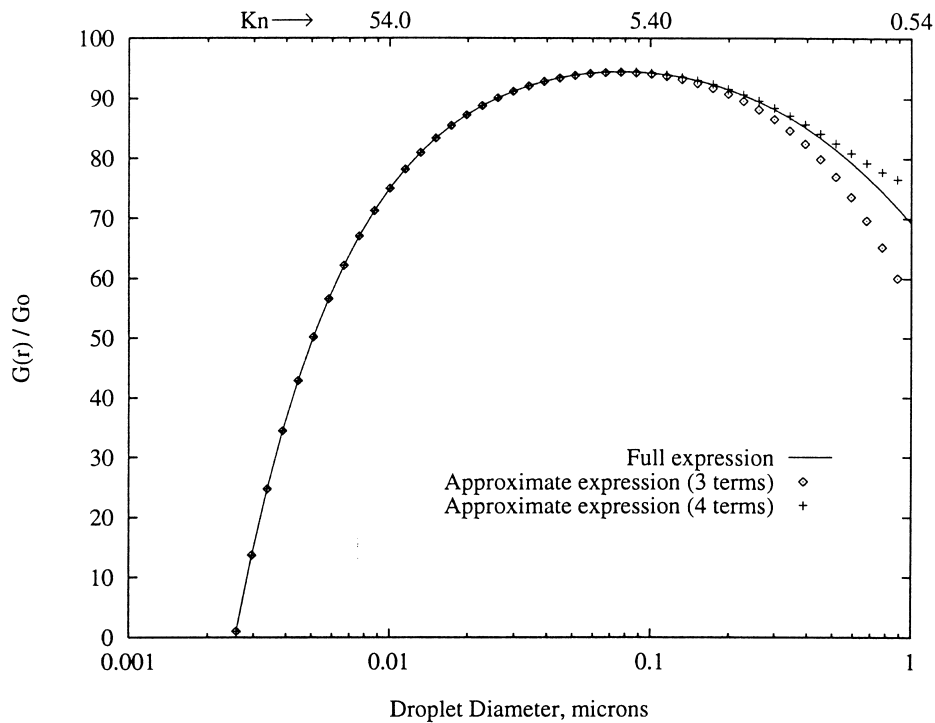


Fig. 8. Comparison of full and approximate growth expressions at  $p = 0.25$  bar and  $\Delta T = 10^\circ\text{C}$ . Note  $G_0$  is the growth rate at a reference radius taken as  $1.1r_*$ .

#### Growth for larger radii or higher pressures

In non-dimensional terms, the growth rate may be expressed as powers of inverse Knudsen number,  $1/Kn = d/l_g$ .  $G/G_0$  then collapses onto a single curve, irrespective of pressure and subcooling, except in the early stages of growth where the  $r/r_*$  term of Eq. (A1) is significant. Values of  $Kn$  are shown along the top axis of Fig. 8. For  $Kn < 0.5$ , i.e., at large radii or high pressures, the truncation errors associated with the expansions shown increase rapidly. This is to be expected since inspection of Eq. (A1) reveals that as  $Kn \rightarrow 0$  (i.e., as the continuum regime is approached),  $G \rightarrow A/r$ , where  $A$  depends on gas properties only. The growth rate can nonetheless be approximated by an expansion of the same form as above by first factoring out  $1/r$  from Eq. (A1). Under such circumstances, the first term in the expansion will dominate, so that a more sophisticated extrapolation for  $\mu_{-1}$  than given by Eq. (23) may be required.

#### References

- [1] J.B. Young, Two-dimensional, non-equilibrium, wet-steam calculations for nozzles and turbine cascades, *Trans. Am. Soc. Mech. Engrs.: J. Turbomachinery* 114 (1992) 569–579.
- [2] P.T. Walters, Improving the accuracy of wetness measurements in generating turbines using a new procedure for analysing optical transmission data, in: *Technology of Turbine Plant Operating with Wet Steam*, British Nuclear Energy Society, London, 1988, pp. 207–215 (Paper 27).
- [3] F. Bakhtar, K.S. So, A study of nucleating flow of steam in a cascade of supersonic blading by the time-marching method, *International Journal of Heat and Fluid Flow* 12 (1991) 54–62.
- [4] A.J. White, J.B. Young, Time marching method for the prediction of two-dimensional, unsteady flows of condensing steam, *AIAA Journal of Propulsion and Power* 9 (4) (1993) 579–587.
- [5] G.H. Schnerr, U. Dohrmann, Theoretical and experimental investigation of 2-D diabatic transonic and supersonic flowfields, in: *Symp. Transonicum III (Göttingen)*, IUTAM Symp, Springer, Berlin, 1988, pp. 132–140.
- [6] M. McCallum, R. Hunt, The flow of wet steam in a one-dimensional nozzle, *Int. J. for Numerical Methods in Engineering* 44 (12) (1999) 1807.
- [7] R. Williams, P.J. Wojtowicz, A simple model for droplet size distribution in atmospheric clouds, *J. Applied Meteorology* 21 (7) (1982) 1042–1044.
- [8] Y.G. Liu, J. Hallett, On size distributions of cloud droplets growing by condensation: a new conceptual

- model, *J. of the Atmospheric Sciences* 55 (4) (1998) 527–536.
- [9] M.J. Hounslow, R.L. Ryall, V.R. Marshall, A discretized population balance for nucleation, growth, and aggregation, *AIChE Journal* 34 (11) (1988) 1821–1831.
- [10] M.J. Hounslow, E.J. W. Wynn, Short-cut models for particulate processes, *Computers and Chem. Eng* 17 (5/6) (1993) 505–516.
- [11] F.A. Williams, *Combustion Theory*. Addison-Wesley, Reading, 1965.
- [12] J.B. Young, The fundamental equations of gas–droplet multiphase flow, *Int. J. Multiphase Flow* 21 (2) (1995) 175–191.
- [13] A.D. Randolph, M.A. Larson, *Theory of Particulate Processes*, Academic Press, New York, 1971.
- [14] H.M. Hulbert, S. Katz, Some problems in particle technology, *Chem. Eng. Sci* 19 (1964) 555–574.
- [15] J.B. Young, The spontaneous condensation of steam in supersonic nozzles, *Physico Chemical Hydrodynamics* 3 (1) (1982) 57–82.
- [16] J.B. Young, Semi-analytical techniques for investigating thermal non-equilibrium effects in wet steam turbines, *Int. J. Heat and Fluid Flow* 5 (2) (1984) 81–91.
- [17] D. Barschdorff, G.A. Phillipov, Analysis of certain special operating modes of laval nozzles with local heat supply, *Heat Transfer — Soviet Research* 2 (5) (1970) 76–87.
- [18] A.J. White, J.B. Young, P.T. Walters, Experimental validation of condensing flow theory for a stationary cascade of steam turbine blades, *Phil. Trans. Roy. Soc* 354 (1996) 59–88.